High expression of six-transmembrane epithelial antigen of prostate 3 promotes the migration and invasion and predicts unfavorable prognosis in glioma

Langmei Deng[1], Shuangshuang Zeng[2], Qiaoli Yi[2] and Liying Song[3]

[1] Department of Emergency, The Third Xiangya Hospital, Central South University, Changsha, Hunan, China
[2] Department of Pharmacy, Xiangya Hospital, Central South University, Changsha, Hunan, China
[3] Department of Pharmacy, The Third Xiangya Hospital, Central South University, Changsha, Hunan, China

Corresponding authors
Qiaoli Yi, yql2019@csu.edu.cn
Liying Song, 602520@csu.edu.cn

ABSTRACT

Recent studies have suggested that ferroptosis, a form of iron-dependent regulated cell death, might play essential roles in tumor initiation and progression. Six-transmembrane epithelial antigen of prostate 3 (STEAP3) is a ferrireductase involved in the regulation of intracellular iron homeostasis. However, the clinical significance and biological function of STEAP3 in human cancers remain poorly understood. Through a comprehensive bioinformatics analysis, we found that STEAP3 mRNA and protein expression were up-regulated in GBM, LUAD, and UCEC, and down-regulated in LIHC. Survival analysis indicated that STEAP3 had prognostic significance only in glioma. Multivariate Cox regression analysis revealed that high STEPA3 expression was correlated with poor prognosis. STEAP3 expression was significantly negatively correlated with promoter methylation level, and patients with lower STEAP3 methylation level had worse prognosis than those with higher STEAP3 methylation level. Single-cell functional state atlas showed that STEAP3 regulated epithelial-to-mesenchymal transition (EMT) in GBM. Furthermore, the results of wound healing and transwell invasion assays demonstrated that knocking down STEAP3 inhibited the migration and invasion of T98G and U251 cells. Functional enrichment analysis suggested that genes co-expressed with STEAP3 mainly participated in inflammation and immune-related pathways. Immunological analysis revealed that STEAP3 expression was significantly correlated with immune infiltration cells, including macrophages and neutrophils, especially the M2 macrophages. Individuals with low STEAP3 expression were more likely to respond to immunotherapy than those with high STEAP3 expression. These results suggest that STEAP3 promotes glioma progression and highlight its pivotal role in regulating immune microenvironment.

INTRODUCTION

Glioma is the most common and fatal primary central nervous system tumor, characterized by a poor prognosis, with a 5-year overall survival rate of only 6.8% for high-grade glioma due to limited effectiveness of surgical resection and chemoradiotherapy (*Magalhaes et al., 2021*; *Thorbinson & Kilday, 2021*; *Zhang et al., 2021b*). Isocitrate dehydrogenase (IDH) mutations and chromosome arms 1p and 19q co-deletion have been identified as molecular pathological markers in glioma, indicating a significant survival benefit (*Ceccarelli et al., 2016*; *Louis et al., 2021*). However, due to the highly invasive and infiltrative nature of glioma cells, current therapeutic regimes and disease monitoring means have achieved limited clinical success (*Magalhaes et al., 2021*; *Xu et al., 2021*). There is an urgent need to identify novel biomarkers for early diagnosis and prognosis prediction in glioma patients.

Six-transmembrane epithelial antigen of prostate 3 (STEAP3) is located on chromosome 2q14.2 and encodes a multi-pass transmembrane protein that acts as an iron transporter. STEAP3 can reduce iron from Fe^{3+} to Fe^{2+} state, and plays an essential role in mediating intracellular iron homeostasis (*Ohgami et al., 2005*; *Ohgami et al., 2006*). The dysregulation of iron metabolism is tightly linked with ferroptosis, a form of regulated cell death modality induced by iron-dependent phospholipids peroxidation on cellular membranes (*Lei, Zhuang & Gan, 2022*). *Liu et al. (2021)* identified that STEAP3 knockdown blocked erastin or RSL3-induced ferroptosis. Accumulating evidence has implicated that ferroptosis participates in the development of diverse cancer types and affects the response to therapies (*Chen et al., 2021b*; *Qu, Peng & Liu, 2022*). Mesenchymal and dedifferentiated tumor cells, associated with resistance to common therapeutics, are susceptible to ferroptosis inducers (*Tsoi et al., 2018*; *Viswanathan et al., 2017*). Ferroptosis induction might be a promising strategy for cancer treatment.

In order to explore the role of STEAP3 in glioma, we first comprehensively analyzed STEAP3 expression profiles, methylation, and its clinical implications with datasets acquired from The Cancer Genome Atlas (TCGA) and the Chinese Glioma Genome Atlas (CGGA). Gene Ontology (GO) and Kyoto Encyclopedia of Genes and Genomes (KEGG) pathway analyses were used to explore the potential molecular mechanisms of STEAP3 and its co-expressed genes. In addition, we analyzed the correlation between STEAP3 expression and immune infiltration. In general, our study indicated that STEAP3 might function as a potential prognostic biomarker in gliomas through immune regulation.

MATERIALS AND METHODS

Gene expression and survival analysis

The integrative bioinformatics analysis of STEAP3 in multiple cancer types was achieved with several bioinformatics databases (Table 1). Tumor Immune Estimation Resource (TIMER2.0) is a web portal for systematical analysis of immune infiltration across various cancer types (*Li et al., 2020*). We used the Gene_DE module of TIMER2.0 to explore the differential expression of STEAP3 gene between tumor samples and normal tissues. Gene expression levels were normalized by log2 (transcripts per million, TPM) prior to analysis.

Table 1 Integrative bioinformatics analyzed in the study.

Database	URL	References
TIMER2.0	http://timer.cistrome.org/	Li et al. (2020)
UALCAN	http://ualcan.path.uab.edu/	Chandrashekar et al. (2017)
HPA	https://www.proteinatlas.org/	Uhlen et al. (2017)
CGGA	http://www.cgga.org.cn/	Zhao et al. (2021b)
CancerSEA	http://biocc.hrbmu.edu.cn/CancerSEA/home.jsp	Yuan et al. (2019)
LinkedOmics	http://linkedomics.org/login.php	Vasaikar et al. (2018)
TISIDB	http://cis.hku.hk/TISIDB	Ru et al. (2019)
TIDE	http://tide.dfci.harvard.edu/	Fu et al. (2020)

For certain tumor types without adjacent normal tissues, the Xiantao tool (https://www.xiantao.love/products) was further applied to explore the differences in STEAP3 expression between TCGA cancer samples and matched TCGA normal tissues and data from the Genotype-Tissue Expression (GTEx) database. Gene expression levels were normalized by log2 (TPM + 1). Through the Xiantao tool, comprehensive bioinformatics analysis can be performed across diverse cancer types, including differential expression analysis, interaction network, functional enrichment analysis, *etc*. Univariate and multivariate Cox regression analysis were carried out to assess the effects of the independent variables on survival using the Xiantao tool. In addition, we also employed the Xiantao tool to assess the prognostic value of STEAP3 in different cancer types. The main outcomes included overall survival (OS), disease-specific survival (DSS), and progression-free survival (PFS). Median STEAP3 expression served as a cutoff to discriminate high- and low-expression groups.

The University of Alabama at Birmingham cancer data analysis portal (UALCAN) is an open-access online database for analyzing cancer omics data (*Chandrashekar et al., 2017*). The protein expression of STEAP3 was explored using data from the Clinical Proteomic Tumor Analysis Consortium (CPTAC) dataset (*Chen et al., 2019*). Immunohistochemistry (IHC) staining was performed to assess the differential expression of STEAP3 at the protein level. The Human Protein Atlas (HPA) (*Uhlen et al., 2017*) was applied to evaluate STEAP3 protein expression in tumor samples and the corresponding normal tissues.

DNA methylation analysis

Aberrant DNA methylation is associated with gene expression, and impacts outcomes for patients with cancer (*Pogribna & Hammons, 2021*). CGGA is a web application that provides correlation and survival analysis in Chinese glioma cohorts based on mRNA expression and DNA methylation data (*Zhao et al., 2021b*). The demographic distribution of STEAP3 methylation and its prognostic value in glioma were analyzed by CGGA. The Xiantao tool was applied to explore the correlation between the expression level of STEAP3 and its promoter DNA methylation degree. Promoter was defined as the 2.1 kb surrounding the transcription start site (TSS) (−2,000 bp/+100 bp) of RefSeq genes.

Single cell sequencing data analysis and gene set enrichment analysis (GSEA)

The Cancer Single-cell State Atlas database (CancerSEA) (*Yuan et al., 2019*) was applied to explore the relevance of STEAP3 across 14 functional states in various cancer types. We downloaded the correlation data and then generated the heatmap. The LinkedOmics database is an open-access portal containing multi-omics data across different cancer types and features three analysis modules: LinkFinder, LinkInterpreter, and LinkCompare (*Vasaikar et al., 2018*). Heatmaps of the top 50 genes positively or negatively correlated with STEAP3 were generated with the LinkFinder module. Furthermore, the LinkInterpreter module was used to perform the GO-biological process (GO-BP) and KEGG pathway analysis.

Tumor immune infiltrate analysis and prediction of immunotherapy responses

The interaction between glioma and immune system were performed using the Xiantao tool and the TISIDB database (*Ru et al., 2019*). First, we used the Xiantao tool to generate the Lollipop diagrams of 24 immune cell types in the TCGA-GBMLGG dataset. Then, the relations between STEAP3 expression and abundance of tumor-infiltrating immune cells were cross-validated using the TISIDB database. In addition, the immune score of each glioma sample was estimated using the "ESTIMATE" R package based on expression data (*Yoshihara et al., 2013*). The relationship between STEAP3 expression and immune score was visualized with scatterplot. We divided glioma patients into high and low immune score groups based on the median values of immune score, and then assessed the prognostic value of immune score in glioma.

Immune checkpoint proteins, such as programmed cell death protein 1 (PD-1), programmed cell death 1 ligand 1 (PD-L1) and cytotoxic T-lymphocyte associated protein 4 (CTLA4), play a critical role in tumor immune escape. Immune checkpoint inhibitors (ICI)-based immunotherapy could produce potent and durable antitumor response (*Kraehenbuehl et al., 2022*). The tumor immune dysfunction and exclusion (TIDE) algorithm was applied to predict the immunotherapy response of glioma patients based on pre-treatment expression profiles (*Fu et al., 2020*).

Cell cultures, reagents, and small interfering RNAs (siRNAs) transfections

Human GBM cell lines T98G and U251 were gifted from the Cancer Research Institute of the Central South University (Changsha, China), as described in our previous study (*Yi et al., 2022*). Two GBM cell lines were incubated in DMEM (C11995500; HyClone, Logan, UT, USA) supplemented with 10% fetal bovine serum (11570506; Gibco, Billings, MT, USA) and 1% penicillin and streptomycin (10378016; Gibco, Billings, MT, USA) at 37 °C with 5% CO_2. For transient transfection, cells were plated in complete serum-containing medium the day before transfection, then transfected with siRNAs of STEAP3 using Lipofectamine™ 3000 Reagent (L3000075, Invitrogen, Waltham, MA, USA) in DMEM. Two STEAP3 siRNAs were purchased form Genechem company (Si1,

GTCTGCTTCTATGCCTACA; Si2, CCCTCTACAGCTTCTGCTT). A total of 8 h after transfection, the serum-free medium was replaced with complete serum-containing medium, and cells were collected 24 h after transfection for subsequent experimental studies.

Western blot

The glioma cells transfected with siNC or STEAP3 siRNAs were lysed with RIPA buffer supplemented with protease inhibitor cocktails (B14012; Bimake, Houston, TX, USA). The BCA protein assay kit (23229; Thermo Fisher Scientific, Waltham, MA, USA) was applied to determine protein concentrations. Protein was transferred into 0.45 μm PVDF membranes (IPVH00010; Millipore, Burlington, MA, USA) after SDS-polyacrylamide gel electrophoresis. Then, the membranes were blocked with 5% nonfat dry milk for 1 h at room temperature. Primary antibodies against STEAP3 (PA5-20406; Thermo Fisher Scientific, Waltham, MA, USA) and β-actin (sc-58673; Santa, Dallas, TX, USA) was incubated overnight at 4 °C. The protein bands were visualized with Immobilon Western chemiluminescent HRP reagents (WBKLS0500; Millipore, Burlington, MA, USA).

Wound healing and transwell invasion assay

Changes in migration and invasion abilities were examined by wound healing and invasion assays, respectively. T98G and U251 cells were cultured to complete confluence in medium containing 10% FBS. The linear wound was created using a plastic scraper. After washed twice with PBS, the medium was replaced with serum-free medium and cultured at 37 °C for 24 h. Then, the wound was observed under a microscope at 0, 12 and 24 h (Olympus, Tokyo, Japan). In invasion assay, Matrigel was purchased from BD Biosciences and thawed overnight at 4 °C. Take 30 μl of Matrigel diluted in serum-free DMEM and inoculate evenly into the upper chamber at 37 °C. Assays were performed using Transwell chambers (8 μm pore-size; Corning, Corning, NY, USA). The lower chambers were loaded with 600 μl of DMEM with 20% FBS. After 24 h of incubation, invaded cells were fixed with 4% paraformaldehyde and stained with 5% crystal violet. Cells on the lower surface of the membrane were counted under a microscope (Olympus, Tokyo, Japan).

Statistical analysis

All experiments and assays were conducted and repeated at least three times, and results were presented as mean ± standard deviation (SD). Statistically significant differences were performed using the T-test or Wilcoxon test for pairwise comparisons or ANOVA for multivariate analysis. Kaplan–Meier survival curves were performed by the log-rank test. Correlation was analyzed using Spearman test. Based on the expression data, the immune score for each glioma sample was estimated using the "ESTIMATE" R package. GraphPad Prism 8 software was used for statistical analysis and $P < 0.05$ was considered as significance.

RESULTS

Expression level of STEAP3 in pan-cancer

We used the TIMER2.0 database to explore the differential expression of STEAP3 between tumor samples and adjacent normal tissues. The flowchart was provided in Fig. S1. As shown in Fig. 1A, significantly differential expression of STEAP3 was found in 16 cancer types, with 11 tumor types up-regulated (BLCA, CESC, GBM, HNSC, LUAD, LUSC, PCPG, READ, STAD, THCA, and UCEC), and five tumor types down-regulated (BRCA, CHOL, KICH, LIHC, and PRAD). For certain cancer types without matched normal tissues in the TMIER2.0 database, we further explored the expression profile of STEAP3 using the Xiantao tool. Compared with the TCGA normal tissues and GTEx data, STEAP3 expression was down-regulated in ACC, CHOL, KICH, LIHC, PRAD, and SKCM, up-regulated in BLCA, CESC, COAD, DLBC, ESCA, GBM, HNSC, KIRC, KIRP, LAML, LGG, LUAD, LUSC, OV, PAAD, PCPG, READ, STAD, TGCT, THCA, THYM, UCEC, and UCS (Fig. 1B). In general, the expression of STEAP3 was elevated in the majority of 32 TCGA tumor types.

Besides transcript levels, using the CPTAC dataset, we further verified that the levels of STEAP3 protein were significantly higher in HNSC, GBM, LUAD, and UCEC samples than in normal tissues, while the levels in LIHC were lower than in normal tissues (Fig. 1C). Then we evaluated immunohistochemical (IHC) staining of STEAP3 proteins in tumor samples and normal tissues using the HPA database. Consistent with protein expression levels in the UALCAN data portal, IHC results revealed that liver tissues had strong STEAP3 IHC staining, while LIHC samples had weak staining. Normal brain, lung, and uterine tissues showed weak or moderate STEAP3 IHC staining, while GBM, LUAD, and UCEC samples exhibited moderate or strong staining (Fig. 1D). However, there was no clear difference in staining intensity between normal tonsil tissue and HNSC (Fig. S2).

The prognostic value of STEAP3 and its correlation with clinicopathological characteristics in glioma

To assess the clinical significance of STEAP3 expression in GBM, LUAD, UCEC, and LIHC, we performed Kaplan-Meier survival analysis for overall survival (OS), disease-specific survival (DSS), and progression-free survival (PFS) with the Xiantao tool. The results showed that high expression of STEAP3 was associated with poor OS (HR = 1.44; 95% CI [1.03–2.03]; P = 0.035) and poor PFS (HR = 1.66; 95% CI [1.18–2.33]; P = 0.004) in GBM (Fig. S3A). Given the lack of normal control tissues in the TCGA-LGG cohort, we added GTEx data to identify the high expression of STEAP3 in LGG. Then we explored the prognostic value of STEAP3 in LGG. As shown in Fig.S3B, patients with higher STEAP3 expression levels had significantly poorer OS (HR = 2.52; 95% CI [1.74–3.63]; P < 0.001), DSS (HR = 2.90; 95% CI [1.95–4.30]; P < 0.001), and PFS (HR = 2.30; 95% CI [1.73–3.06]; P < 0.001). Considering the consistent prognostic significance of STEAP3 in GBM and LGG, we further evaluated the prognostic value of STEAP3 in glioma. As presented in Fig. 2A, high expression levels of STEAP3 also correlated with poorer OS (HR = 5.44; 95% CI [4.09–7.24]; P < 0.001), DSS (HR = 5.87;
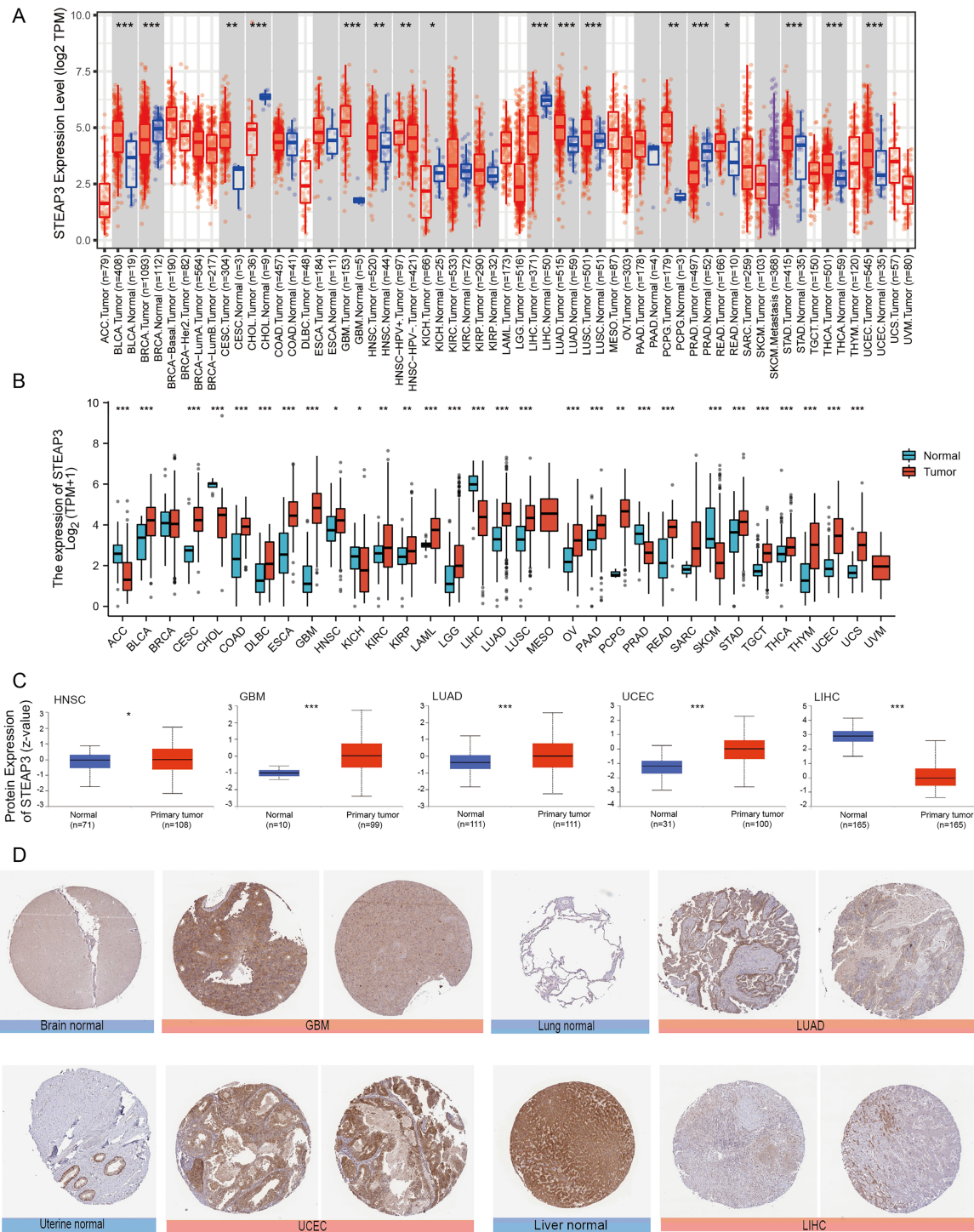
Figure 1 Expression level of STEAP3 in pan-cancer. (A) The mRNA expression levels of STEAP3 in TCGA cancer types from the TIMER2.0 database. Red and blue bar charts represent tumor samples and normal tissues, respectively. (B) Pan-cancer expression landscape of STEAP3 across TCGA and GTEx data from the Xiantao database. (C) The protein expression levels of STEAP3 in HNSC, GBM, LUAD, UCEC, and LIHC, analyzed by CPTAC. (D) The immunohistochemical analysis performed on GBM, LUAD, UCEC, and LIHC and corresponding normal tissues using the HPA database. *P* values: * represents *P* < 0.05, ** represents *P* < 0.01, and *** represents *P* < 0.001.

95% CI [4.32–7.96]; *P* < 0.001), and PFS (HR = 3.71; 95% CI [2.95–4.67]; *P* < 0.001). Kaplan-Meier survival analysis showed no statistical significance of STEAP3 in LUAD, UCEC, and LIHC (Figs. 2B–2D). Therefore, we mainly studied the effect of STEAP3 in glioma.

Univariate Cox regression analysis of seven independent variables in TCGA-GBMLGG cohort was carried out. Age, WHO grade, IDH status, 1p/19q co-deletion, and STEAP3 expression level, demonstrated a significant prognostic impact on OS. Multivariate Cox regression analysis exhibited that age (HR = 1.496; 95% CI [1.096–2.042]; *P* = 0.011), WHO grade (HR = 2.622; 95% CI [1.828–3.760]; *P* < 0.001), IDH status (HR = 0.305; 95% CI [0.198–0.470]; *P* < 0.001), and STEAP3 expression level (HR = 1.673; 95% CI [1.110–2.522]; *P* = 0.014) were independent prognostic factors for glioma patients (Table 2). Univariate Cox regression analysis also suggested an association between PFS and age, WHO grade, IDH status, 1p/19q co-deletion, and STEAP3 expression level. Multivariate Cox regression analysis indicated that WHO grade (HR = 1.974; 95% CI [1.435–2.716]; *P* < 0.001), IDH status (HR = 0.290; 95% CI [0.200–0.421]; *P* < 0.001), and STEAP3 expression level (HR = 1.450; 95% CI [1.045–2.013]; *P* = 0.026) were independent prognostic factors for glioma patients (Table 3). These results suggest that higher STEAP3 expression was associated with worse prognosis.

Furthermore, we employed the RNAseq_693 dataset from CGGA database to cross-validate the role of STEAP3 in glioma. STEAP3 expression was markedly elevated in high-grade and recurrent glioma patients (Figs. 3A and 3B). IDH mutation and 1p/19q co-deletion are two validated biomarkers for glioma patients. We then explored the association between STEAP3 expression and the status of IDH mutation and 1p/19q co-deletion. As shown in Figs. 3C–3G, we found significantly increased STEAP3 expression in patients with IDH wild-type and 1p/19q non-codeletion, and correlated with WHO grade. In addition, patients older than 42 years harbored higher STEAP3 expression levels (Fig. 3H). Patients with higher STEAP3 expression had worse prognosis than those with lower STEAP3 expression in primary and recurrent gliomas, respectively (Figs. 3I and 3J). These findings further validated the prognostic value of STEAP3 and its correlation with clinicopathological parameters in glioma.

DNA methylation of STEAP3 and its prognostic value in glioma

Epigenetic changes, such as aberrant DNA methylation, commonly contribute to the development of human tumors, including brain glioma (*Russo et al., 2021*). We explored the DNA methylation pattern of STEAP3 in the Methyl_159 dataset of CGGA database. The methylation level of STEAP3 was obviously decreased with WHO grade (Fig. 4A). STEAP3 methylation levels were significantly reduced in male patients (Fig. 4B). In primary gliomas, patients with lower STEAP3 methylation level had worse prognosis than those with higher STEAP3 methylation level (Fig. 4C). These results were consistent with STEAP3 expression data. Furthermore, we employed the Xiantao tool to explore the correlation between STEAP3 expression and the degree of DNA methylation at multiple CpG sites. As shown in Figs. 4D–4I, cg05270572, cg23164999, cg25845374, cg18643762, cg04749104, and cg25101327, were significantly negatively correlated with STEAP3
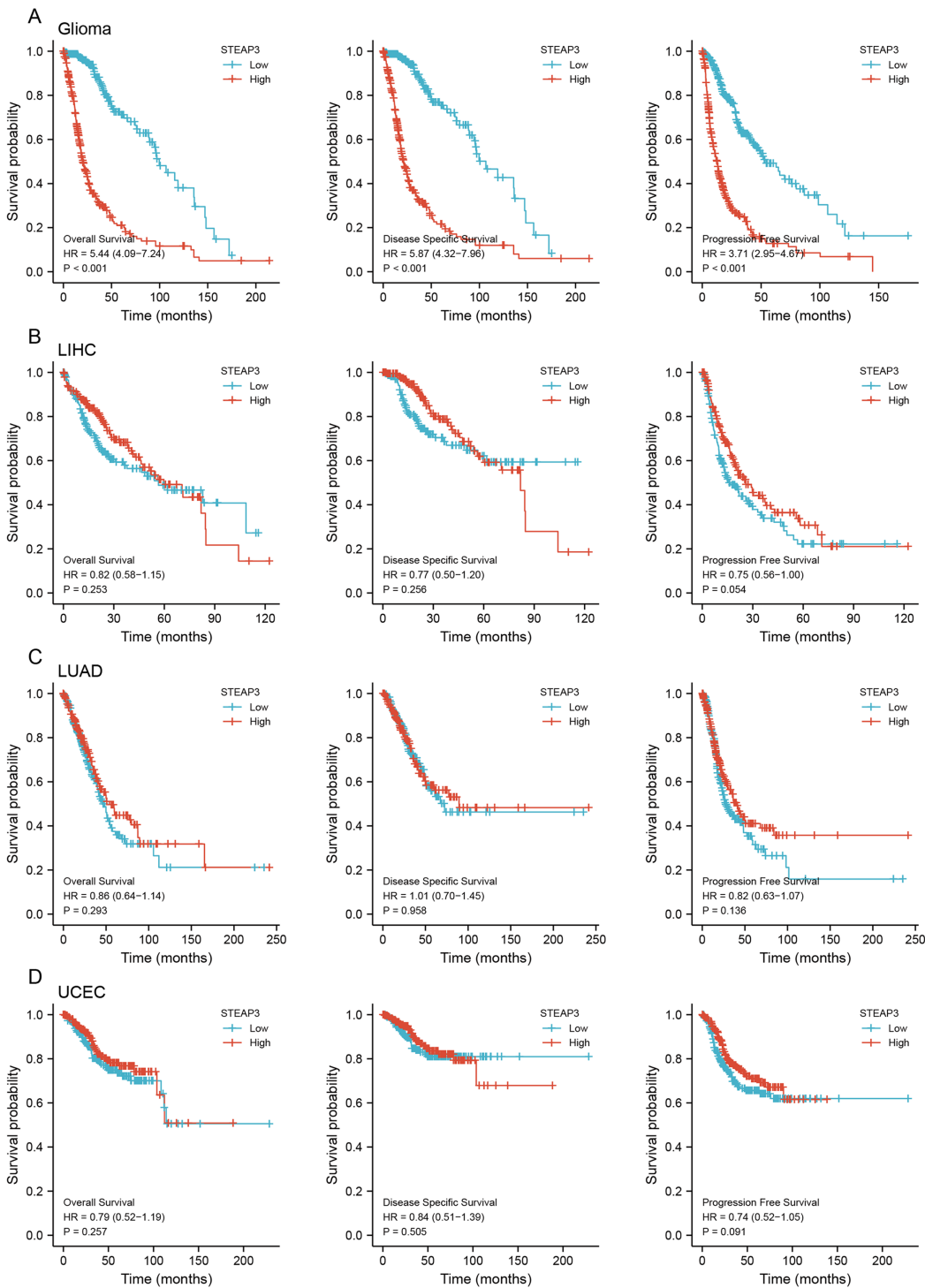
Figure 2 Prognostic value of STEAP3 in glioma, LIHC, LUAD, and UCEC. (A–D) Kaplan-Meier survival curves for overall survival, disease-specific survival, and progression free survival of STEAP3 in glioma (A), LIHC (B), LUAD (C), and UCEC (D).

Table 2 Univariate and multivariable Cox regression of STEAP3 expression for overall survival in TCGA-GBMLGG cohorts.

Characteristics	Univariate Cox regression		Multivariate Cox regression	
	Hazard ratio (95% CI)	P value	Hazard ratio (95% CI)	P value
WHO grade: G2 & G3 vs G4	9.496 [7.212–12.503]	**<0.001**	2.622 [1.828–3.760]	**<0.001**
IDH status: WT vs Mut	0.117 [0.090–0.152]	**<0.001**	0.305 [0.198–0.470]	**<0.001**
1p/19q codeletion: codel vs non-codel	4.428 [2.885–6.799]	**<0.001**	1.467 [0.887–2.428]	0.136
Gender: Female vs Male	1.262 [0.988–1.610]	0.062	1.223 [0.934–1.602]	0.144
Race: Asian & Black or African American vs White	0.821 [0.502–1.344]	0.433		
Age: <=60 vs >60	4.668 [3.598–6.056]	**<0.001**	1.496 [1.096–2.042]	**0.011**
STEAP3: Low vs High	5.440 [4.088–7.240]	**<0.001**	1.673 [1.110–2.522]	**0.014**

Note:
Bold P values are statistically significant (P < 0.05).

Table 3 Univariate and multivariable Cox regression of STEAP3 expression for progression-free survival in TCGA-GBMLGG cohorts.

Characteristics	Univariate Cox regression		Multivariate Cox regression	
	Hazard ratio (95% CI)	P value	Hazard ratio (95% CI)	P value
WHO grade: G2 & G3 vs G4	6.008 [4.726–7.638]	**<0.001**	1.974 [1.435–2.716]	**<0.001**
IDH status: WT vs Mut	0.151 [0.119–0.191]	**<0.001**	0.290 [0.200–0.421]	**<0.001**
1p/19q codeletion: codel vs non-codel	3.373 [2.438–4.666]	**<0.001**	1.446 [0.993–2.106]	0.055
Gender: Female vs Male	1.083 [0.875–1.342]	0.463		
Race: Asian & Black or African American vs White	0.787 [0.515–1.202]	0.267		
Age: <=60 vs >60	2.873 [2.268–3.640]	**<0.001**	1.044 [0.781–1.395]	0.772
STEAP3: Low vs High	3.708 [2.947–4.666]	**<0.001**	1.450 [1.045–2.013]	**0.026**

Note:
Bold P values are statistically significant (P < 0.05).

expression in glioma. A gene structure plot illustrating the position of the CpG sites was shown in Fig. S4. These results revealed that STEAP3 promoter methylation was inversely correlated with its gene expression, and might serve as an effective prognostic biomarker for glioma.

Single-cell functional state atlas of STEAP3 in glioma

Considering the intra-tumoral heterogeneity, we continued to explore the relevance of STEAP3 expression across 14 functional states in cancers at single-cell resolution. STEAP3 expression was significantly positively associated with epithelial-to-mesenchymal transition (EMT) in GBM, but not all glioma types (Figs. 5A and 5B). These results suggested that STEAP3 might promote the EMT process of GBM, thus facilitating tumor invasion and metastasis. To further confirm the effects of STEAP3 in glioma, wound healing and transwell invasion assays were conducted. Transient transfection of STEAP3 was established by siRNAs and validated by Western Blot (Fig. 5C). The results of wound healing assays revealed that knocking down of STEAP3 could significantly suppress glioma cells migration (Figs. 5D and 5E). Transwell invasion assays revealed that STEAP3 downregulation remarkably inhibit T98G and U251 cells invasion (Figs. 5F and 5G).
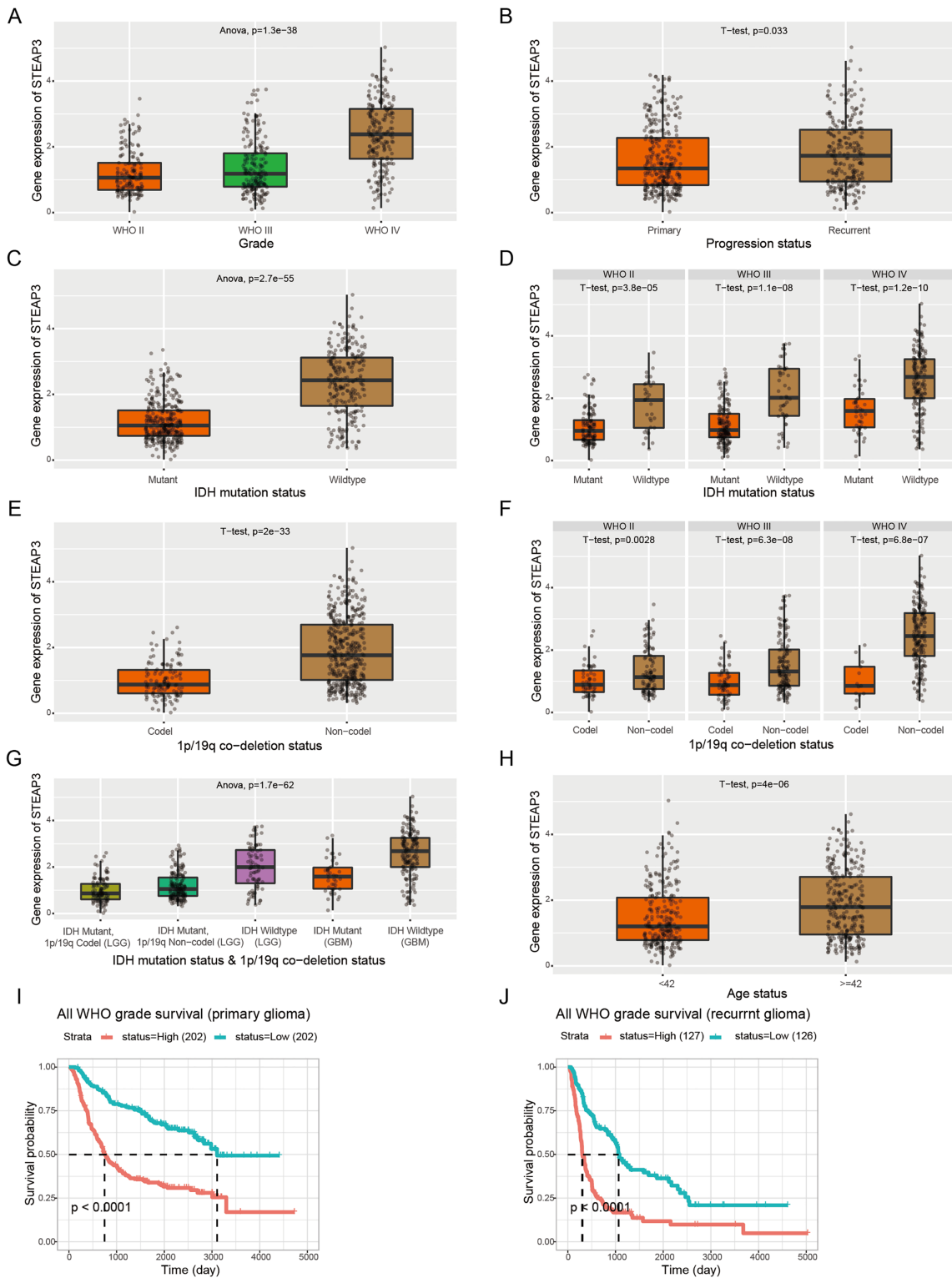
Figure 3 Correlation between STEAP3 expression and clinicopathological characteristics in glioma. (A–J) Correlation of STEAP3 expression level with WHO grade (A), progression status (B), IDH mutation status (C), IDH mutation status based on WHO grade (D), 1p/19q co-deletion status (E), 1p/19q co-deletion status based on WHO grade (F), combination of IDH mutation status and 1p/19q co-deletion status (G), age status (H), and survivals (I and J) from the RNAseq_693 dataset in CGGA database.
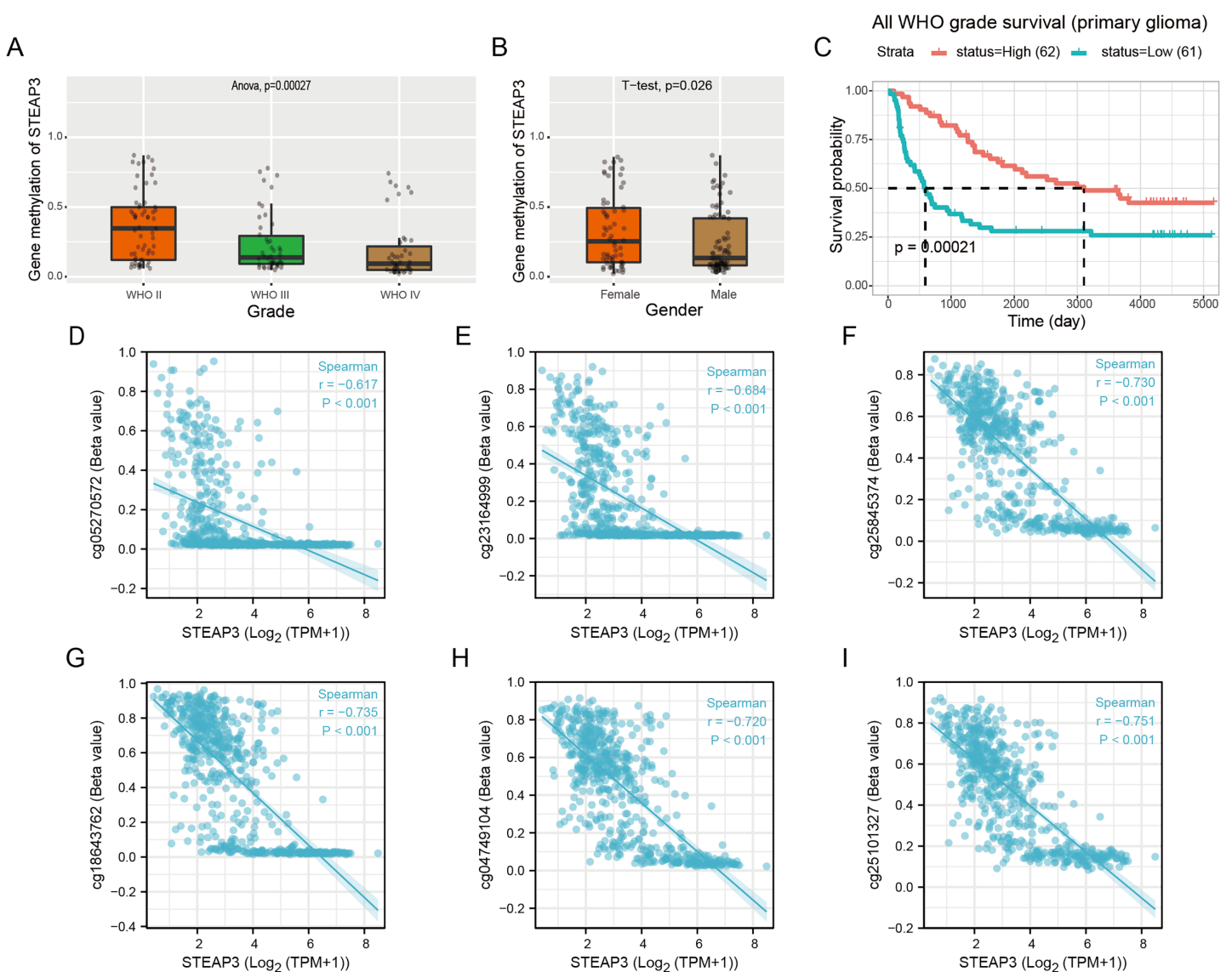
Figure 4 Correlation between STEAP3 methylation and clinicopathological characteristics in glioma. (A–C) Correlation of STEAP3 methylation level with WHO grade (A), gender (B), and survival (C) from the Methyl_159 dataset in CGGA database. (D–I) Correlation between STEAP3 expression and DNA methylation at CpG sites in the STEAP3 gene by the Xiantao database.

Namely, these observations indicate that STEAP3 facilitated migration and invasion in glioma cells.

STEAP3 co-expression network and pathway enrichment analysis

To investigate the biological roles of STEAP3 in glioma progression, the STEAP3 co-expression profile in the TCGA-GBMLGG cohort was analyzed using the LinkFinder module of LinkedOmics. As presented in Fig. 6A, 8,702 genes (red dots) were positively associated with STEAP3, and 7,816 genes (green dots) were negatively correlated with STEAP3. Figures 6B and 6C showed the heatmaps of the top 50 genes bearing positive and negative correlations with STEAP3, respectively (Table S1). Additionally, genes positively
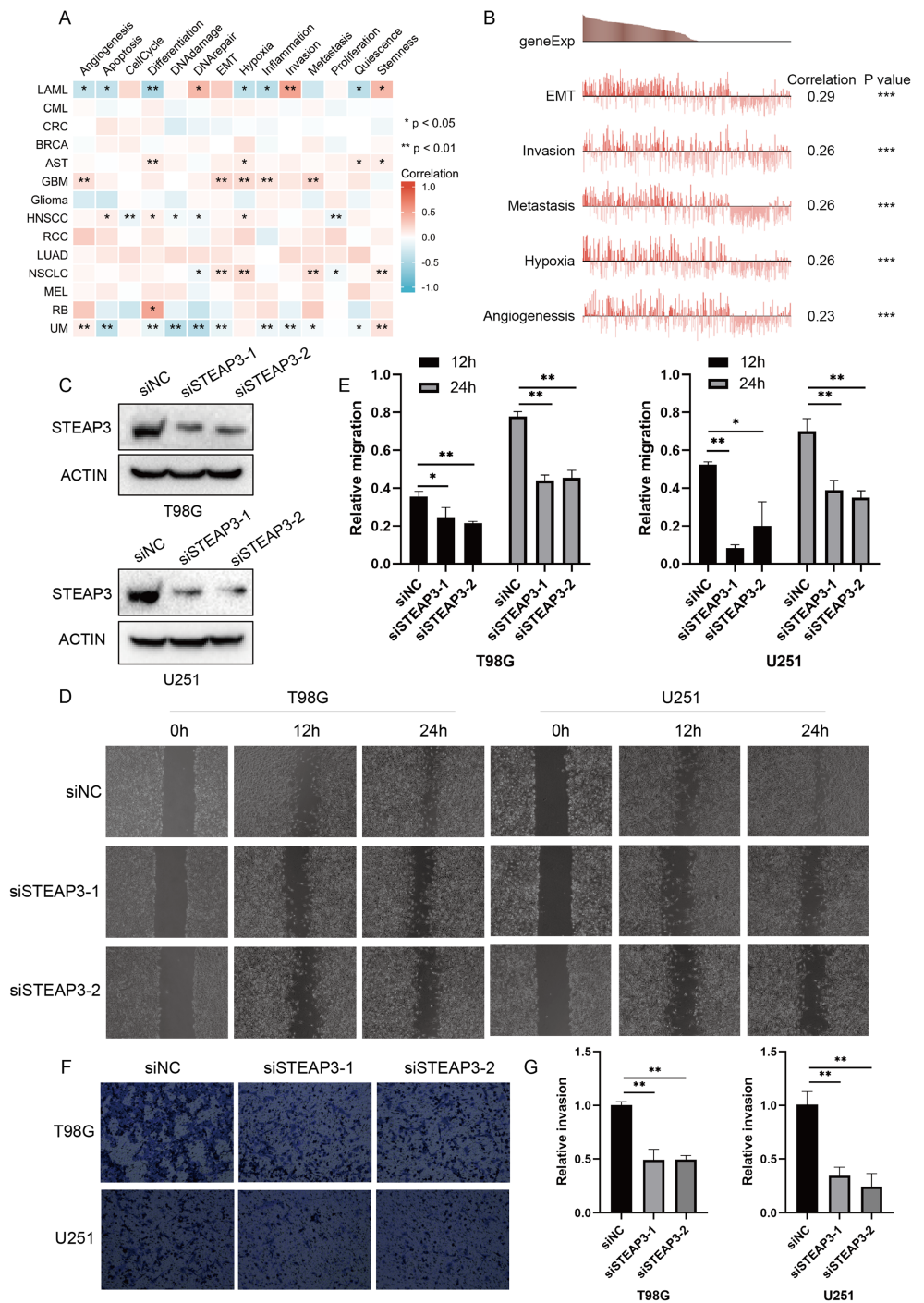
Figure 5 Functional relevance of STEAP3 in glioma. (A) Relevance of STEAP3 across 14 functional states in distinct cancers using the CancerSEA database. Red indicates positive correlation whereas blue represents negative correlation. (B) Functional relevance of STEAP3 in GBM analyzed by the CancerSEA database. (C) Confirmation of siSTEAP3 or siNC-mediated knockdown efficiency of STEAP3 by western blot. (D and E) Scratch assay showed significant migration delay in siSTEAP3 cells at 12, 24 h after transfection compared to siNC cells (T98G and U251). (F and G) Invasion of T98G and U251 cells with siNC or siSTEAP3 transfection was detected through transwell assay. *P* values: * represent *P* < 0.05, ** represent *P* < 0.01, and *** represent *P* < 0.001.
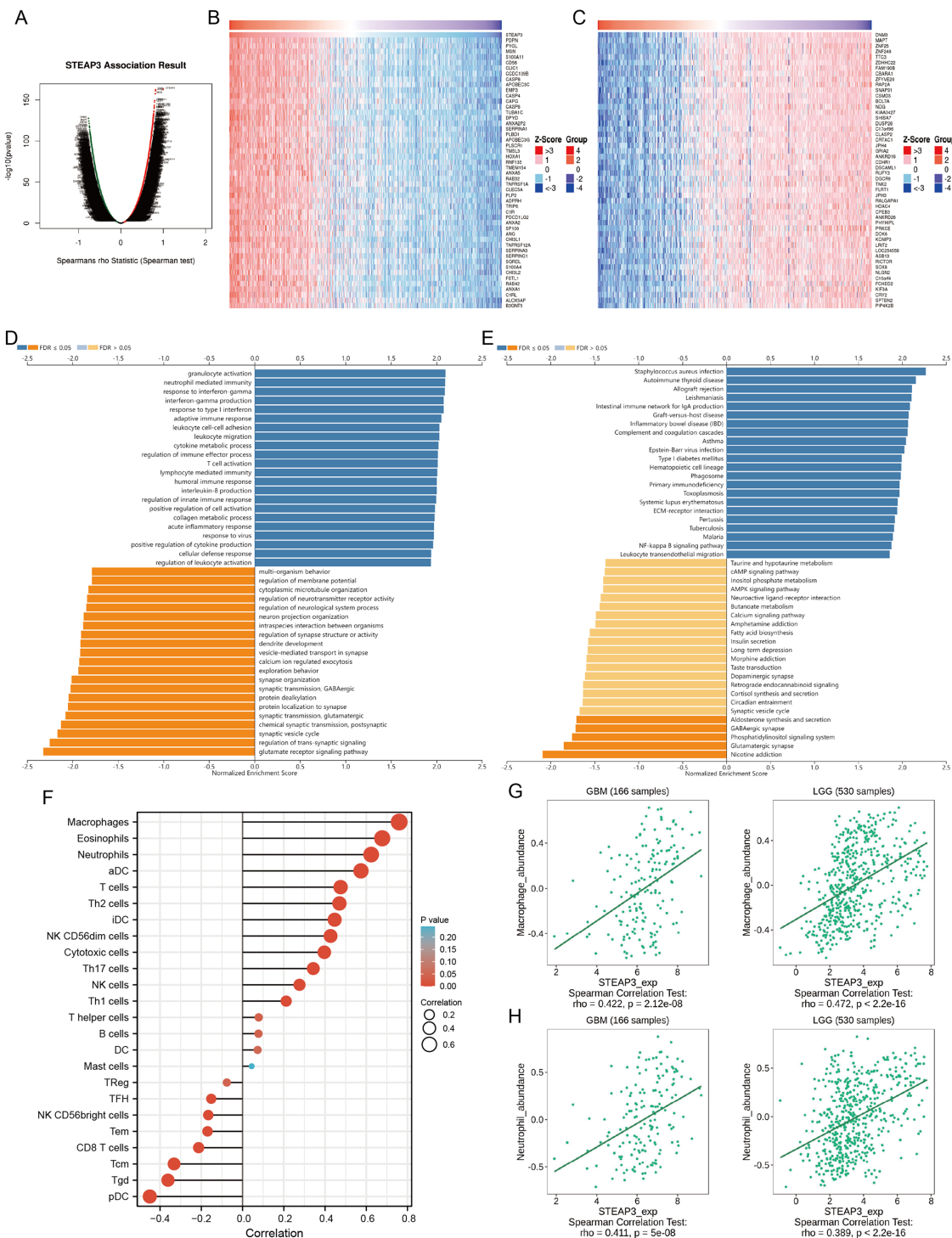
Figure 6 STEAP3 co-expression network and GSEA enrichment analysis. (A) Volcano plot showing the co-expressed profiling of STEAP3 in glioma by Spearman test. (B and C) Heatmaps of the top 50 genes positively (B) and negatively (C) correlated with STEAP3, respectively. (D and E) GO (D) and KEGG (E) pathway analysis of the STEAP3 co-expression genes with the LinkInterpreter module of the LinkedOmics database. (F) The correlation between STEAP3 expression and immune cell infiltration in glioma analyzed by the Xiantao tool. (G and H) Validations of the positive correlation between STEAP3 expression and macrophages (G) and neutrophils (H) in GBM and LGG by the TISIDB database.

associated with STEAP3 ($P < 0.05$, gene counts: 8,702) were subjected to functional enrichment analysis using the LinkInterpreter module. Gene Ontology term annotation suggested that genes co-expressed with STEAP3 were significantly enriched in inflammation and immune-associated biological process, such as granulocyte activation, neutrophil mediated immunity, response to interferon-gamma, interferon-gamma production, adaptive immune response, and so on (Fig. 6D). KEGG pathway analysis exhibited that these genes were mainly involved in inflammation and immune-related pathways, such as *Staphylococcus aureus* infection, autoimmune thyroid disease, allograft rejection, leishmaniasis, intestinal immune network for IgA production, *etc.* (Fig. 6E). These findings suggested that STEAP3 co-expression network may play a role in inflammation and immune regulation in glioma.

Role of STEAP3 in immune microenvironment of glioma

An increasing number of studies have confirmed that ferroptosis plays an important role in regulating tumor immune microenvironment (*Wang et al., 2022*; *Yan et al., 2021*). Therefore, we explored the role of STEAP3 in glioma immune microenvironment. As shown in Fig. 6F, STEAP3 expression was positively correlated with the abundance of various immune infiltration cells, such as macrophages, eosinophils, and neutrophils. The association between STEAP3 expression and macrophages was cross-validated in the TCGA-GBM and TCGA-LGG cohort using TISIDB database, respectively, but not in eosinophils (Figs. 6G and 6H). Using the Xiantao tool, we further analyzed the correlations between STEAP3 with immune checkpoints. As shown in Figs. 7A–7E, immune checkpoints were found to have significant positive correlations with STEAP3, while programmed cell death 1 ligand 2 (PDCD1LG2) exhibited the highest correlation coefficient (r = 0.775, $P < 0.001$). In addition, we assessed the relation between immune infiltration score and STEAP3 expression. Figures 7F and 7G showed its positive association and patients with high immune infiltration score had poorer overall survival (OS) in glioma. We then used the TIDE algorithm to predict anti-PD1 and anti-CTLA4 immunotherapy response in glioma patients. As shown in Fig. 7H, individuals with low STEAP3 expression were more likely to respond to immunotherapy than those with high STEAP3 expression. Consistent with this result, the TIDE score was down-regulated in STEAP3 low expression group, and the microsatellite instability (MSI) score was up-regulated in STEAP3 low expression group (Figs. 7I and 7J). These results indicated that STEAP3 might influence the clinical outcome of glioma patients by regulating the tumor immune microenvironment.

STEAP3 relating with M2 macrophages in glioma

The correlation analysis revealed that STEAP3 expression was significantly positively associated with the abundance of macrophage infiltration. We further explored the associations between STEAP3 expression and classical macrophage phenotype in the TCGA-GBMLGG cohort with Spearman's rank correlation test, including gene expression of M0 (undifferentiated) marker (AIF1), M1 (anti-tumor) markers (IL12A, TNF, NOS2, PTGS2) and M2 (tumor-promoting) markers (IL10, CD163, TGFB1, CSF1R). As shown in
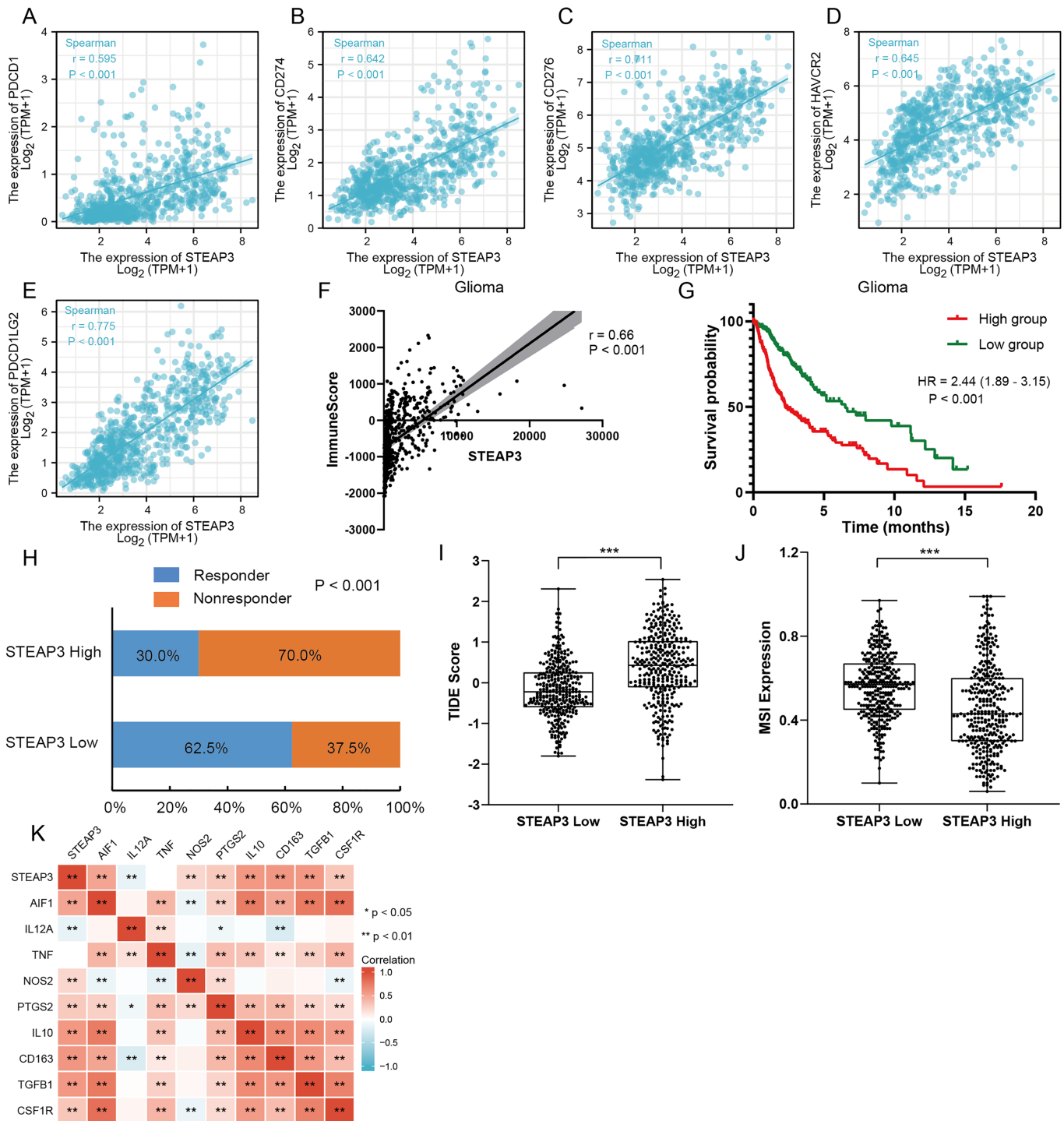
Figure 7 The role of STEAP3 in the immune microenvironment of glioma. (A–E) Correlation of STEAP3 expression and several immune checkpoints, such as PDCD1 (A), CD274 (B), CD276 (C), HAVCR2 (D), PDCD1LG2 (E). (F) Association between STEAP3 expression with immune score in the TCGA glioma dataset calculated by ESTIMATE algorithm. (G) Kaplan–Meier survival curve of overall survival stratified by immune score in the TCGA glioma dataset. (H) Predicted anti-PD1 and anti-CTLA4 response rate for STEAP3 high and low groups in the TCGA glioma dataset. (I and J) TIIDE score (I) and MSI expression (J) between STEAP3 high and low groups. (K) Heatmap of correlation between STEAP3 and classical macrophage phenotype markers. *P* values: * represent $P < 0.05$, ** represent $P < 0.01$, and *** represent $P < 0.001$.

Fig. 7K, STEAP3 had stronger positive correlations with M0 (AIF1) and M2 (IL10, CD163, TGFB1, CSF1R) macrophage markers, but not with M1 (IL12A, TNF, NOS2, PTGS2) markers. These findings suggested that STEAP3 may regulate tumor immune microenvironment by promoting the formation of the M2 macrophages in glioma.

DISCUSSION

In this study, we aimed to investigate the clinical significance and biological function of STEAP3 in the tumorigenesis and progression of glioma. Compared with normal brain tissue, STEAP3 was highly expressed in glioma and was significantly associated with poor prognosis. Furthermore, multivariate Cox regression analysis indicated that STEAP3 was an independent prognostic factor in glioma. STEAP3 promoter hypomethylation may be the mechanism of upregulation in glioma. Further research revealed that STEAP3 may affect tumor immune response by increasing the infiltration level of M2 macrophages.

Recently, accumulating evidence has revealed that ferroptosis plays an essential role in glioma initiation and progression. RND1 (Rho family GTPase 1), a positive regulator of p53, could induce lipid peroxidation and enhance ferroptosis in GBM (*Sun et al., 2022*). *Xia et al. (2022)* identified that apatinib, a small-molecule tyrosine kinase inhibitor, induced ferroptosis in glioma through modulation of the NRF2 pathway, in addition to antiangiogenic and anticancer activities. Additionally, many studies have suggested that ferroptosis induction could be a promising therapeutic strategy (*de Souza et al., 2022b*; *Hu et al., 2020*). In a recent study by *de Souza et al. (2022a)*, high levels of NRF2 could reverse temozolomide resistance in glioma *via* ferroptosis induction. Ferroptosis inducers could enhance the antitumor effect of radiation and may serve as effective radiosensitizers that could expand the efficacy and indications of radiation therapy (*Ye et al., 2020*). However, the link between ferroptosis-related genes and prognosis in glioma patients has been rarely reported. In our study, we explored the prognostic value of ferroptosis-associated gene STEAP3 in glioma, and found that high levels of STEAP3 served as an independent poor prognostic prediction factor in glioma patients.

DNA methylation, a methyl group added to the fifth carbon of the cytosine residue in cytosine-guanine (CpG) dinucleotides, is one of the well-characterized epigenetic mechanisms for regulating gene expression (*Xue et al., 2021*). Accumulating evidence has suggested that altered DNA methylation patterns are associated with a wide range of age-related diseases, including vascular disease (*Lu et al., 2021*), Alzheimer's disease (*Altuna et al., 2019*), and cancer (*Klutstein et al., 2017*). DNA methylation patterns could contribute to tumorigenesis and progression by regulating the expression levels of oncogenes and tumor-suppressor genes (*Costello et al., 2000*; *Pathania et al., 2015*). According to the analysis of TCGA datasets and IHC staining from HPA database, glioma exhibited significantly high STEAP3 mRNA and protein expression. The mechanisms of STEAP3 upregulation in glioma are currently poorly understood. In our study, the DNA methylation levels of STEAP3 in high-grade glioma were significantly lower than those in low-grade glioma, and the methylation levels of multiple methylated CpG sites were significantly negatively correlated with STEAP3 expression, indicating that low levels of
STEAP3 promoter methylation are responsible for the overexpression of STEAP3 in glioma.

The immune microenvironment is composed of various immune cells, cytokines, chemokines, and so on (*Huang et al., 2018*; *Wang et al., 2022*). Emerging studies have suggested that glioma has a suppressive immune microenvironment, which further inhibits the response to immunotherapy represented by anti-PD-1/PD-L1 and anti-CTLA4 (*Jackson, Choi & Lim, 2019*; *Lim et al., 2018*; *Xu et al., 2020*). Tumor-associated macrophages (TAMs), instead of T lymphocytes, are the most abundant immune cell populations involved in glioma development (*Wei et al., 2019*). TAMs in glioma exhibit M2-like macrophage polarization, which largely contributes to the induction of immunosuppressive microenvironment, and further facilitate tumor proliferation, migration, and survival (*Hambardzumyan, Gutmann & Kettenmann, 2016*; *Zhang et al., 2021a*). Colony stimulating factor 1 receptor (CSF1R) inhibition could regulate M2 macrophage polarization and attenuate glioma progression (*Przystal et al., 2021*; *Pyonteck et al., 2013*). CD163, a membrane protein considered as the most specific M2 macrophage phenotypic marker, predicts poor prognosis in patients with glioma (*Liu et al., 2019*). In the present study, the findings showed that M2 macrophage markers CD163 and CSF1R were positively correlated with STEAP3 expression in glioma, suggesting that the function of STEAP3 might be related to the regulation of macrophage M2 polarization. Furthermore, our studies revealed that co-expression genes of STEAP3 might participate in inflammation and immune-associated pathways, and STEAP3 expression was positively associated with immune checkpoints. Additionally, immune infiltration analysis showed that individuals with high immune score had a tendency towards the upregulation of STEAP3, which coupled with worse OS. Patients with high STEAP3 expression were associated with low response rates to immunotherapy. Together these results imply that the role of STEAP3 might be involved in the induction of immunosuppressive environment and may be a promising therapeutic target for glioma immunotherapy.

To date, several studies have reported the prognostic prediction potential of STEAP3 in GBM (*Chen et al., 2021a*; *Han et al., 2018*; *Zhao et al., 2021a*). STEAP3-associated prognostic signatures for glioma have also been reported (*Guo et al., 2021*; *Weston et al., 2016*). However, existing studies on the biological function and molecular mechanisms of STEAP3 in glioma are few in number. *Han et al. (2018)* identified that STEAP3 could promote the growth and invasion of glioblastoma, which was consistent with our findings. The possible mechanism by which STEAP3 promotes glioma progression may be through the activation of TfR and the downstream ferritin-STAT3 pathway. In addition, our study indicated that the methylation of STEAP3 promoter region was highly negatively correlated with its expression. Tumor immune infiltrate analysis showed that STEAP3 might influence the clinical outcome of glioma patients by regulating the tumor immune microenvironment, especially the formation of the M2 macrophages. The CancerSEA database showed that STEAP3 may contribute to glioma progression by promoting EMT. However, the mechanism of this effect remains to be further investigated.

In the present study, several limitations still exist. Firstly, gene expression analysis based on retrospective databases needs further investigations in large-scale prospective clinical

cohorts to confirm the prognostic value of STEAP3 in glioma. Secondly, it is necessary to conduct functional experiments to elaborate the biological mechanism of STEAP3 and tumor-immune interactions in glioma.

CONCLUSION

Taken together, by comprehensively assessing the gene expression profiles, our study provides new insights into the interaction between ferroptosis and glioma immune microenvironment. STEAP3 was up-regulated in glioma, and increased with tumor grade. High STEAP3 expression was recognized as an independent poor prognostic factor. Further study suggested that STEAP3 may contribute to the induction of glioma immunosuppressive microenvironment by regulating macrophage M2 polarization. In summary, STEAP3 has great potential as a prognostic biomarker and therapeutic target in glioma.

ABBREVIATIONS

ACC	adrenocortical carcinoma
BLCA	bladder urothelial carcinoma
BRCA	breast invasive carcinoma
CESC	cervical squamous cell carcinoma and endocervical adenocarcinoma
CHOL	cholangiocarcinoma
COAD	colon adenocarcinoma
DLBC	diffuse large B-cell lymphoma
ESCA	esophageal carcinoma
GBM	glioblastoma multiforme
HNSC	head and neck squamous cell carcinoma
KICH	kidney chromophobe
KIRC	kidney renal clear cell carcinoma
KIRP	kidney renal papillary cell carcinoma
LAML	acute myeloid leukemia
LGG	brain lower grade glioma
LIHC	liver hepatocellular carcinoma
LUAD	lung adenocarcinoma
LUSC	lung squamous cell carcinoma
MESO	mesothelioma
OV	ovarian serous cystadenocarcinoma
PAAD	pancreatic adenocarcinoma
PCPG	pheochromocytoma and paraganglioma
PRAD	prostate adenocarcinoma
READ	rectum adenocarcinoma
SARC	sarcoma
SKCM	skin cutaneous melanoma
STAD	stomach adenocarcinoma

TGCT	testicular germ cell tumors
THCA	thyroid carcinoma
THYM	thymoma
UCEC	uterine *corpus* endometrial carcinoma
UCS	uterine carcinosarcoma
UVM	uveal melanoma

Funding
This study is supported by grants from the Research Fund of the Third Xiangya Hospital. The funders had no role in study design, data collection and analysis, decision to publish, or preparation of the manuscript.

Grant Disclosures
The following grant information was disclosed by the authors:
Research Fund of the Third Xiangya Hospital.

Competing Interests
The authors declare that the research was conducted in the absence of any commercial or financial relationships that could be construed as a potential conflict of interest.

Author Contributions
- Langmei Deng analyzed the data, prepared figures and/or tables, authored or reviewed drafts of the article, and approved the final draft.
- Shuangshuang Zeng conceived and designed the experiments, authored or reviewed drafts of the article, and approved the final draft.
- Qiaoli Yi conceived and designed the experiments, performed the experiments, prepared figures and/or tables, and approved the final draft.
- Liying Song conceived and designed the experiments, authored or reviewed drafts of the article, and approved the final draft.

Data Availability
The raw data is available in the Supplemental Files.

Supplemental Information
Supplemental information for this article can be found online at http://dx.doi.org/10.7717/peerj.15136#supplemental-information.

REFERENCES

Altuna M, Urdanoz-Casado A, Sanchez-Ruiz de Gordoa J, Zelaya MV, Labarga A, Lepesant JMJ, Roldan M, Blanco-Luquin I, Perdones A, Larumbe R, Jerico I, Echavarri C, Mendez-Lopez I, Di Stefano L, Mendioroz M. 2019. DNA methylation signature of human

hippocampus in Alzheimer's disease is linked to neurogenesis. *Clinical Epigenetics* **11**(1):91 DOI 10.1186/s13148-019-0672-7.

Ceccarelli M, Barthel FP, Malta TM, Sabedot TS, Salama SR, Murray BA, Morozova O, Newton Y, Radenbaugh A, Pagnotta SM, Anjum S, Wang J, Manyam G, Zoppoli P, Ling S, Rao AA, Grifford M, Cherniack AD, Zhang H, Poisson L, Carlotti CG Jr, Tirapelli DP, Rao A, Mikkelsen T, Lau CC, Yung WK, Rabadan R, Huse J, Brat DJ, Lehman NL, Barnholtz-Sloan JS, Zheng S, Hess K, Rao G, Meyerson M, Beroukhim R, Cooper L, Akbani R, Wrensch M, Haussler D, Aldape KD, Laird PW, Gutmann DH, Network TR, Noushmehr H, Iavarone A, Verhaak RG. 2016. Molecular profiling reveals biologically discrete subsets and pathways of progression in diffuse glioma. *Cell* **164**(3):550–563 DOI 10.1016/j.cell.2015.12.028.

Chandrashekar DS, Bashel B, Balasubramanya SAH, Creighton CJ, Ponce-Rodriguez I, Chakravarthi B, Varambally S. 2017. UALCAN: a portal for facilitating tumor subgroup gene expression and survival analyses. *Neoplasia* **19**(8):649–658 DOI 10.1016/j.neo.2017.05.002.

Chen F, Chandrashekar DS, Varambally S, Creighton CJ. 2019. Pan-cancer molecular subtypes revealed by mass-spectrometry-based proteomic characterization of more than 500 human cancers. *Nature Communications* **10**(1):5679 DOI 10.1038/s41467-019-13528-0.

Chen X, Kang R, Kroemer G, Tang D. 2021b. Broadening horizons: the role of ferroptosis in cancer. *Nature Reviews Clinical Oncology* **18**(5):280–296 DOI 10.1038/s41571-020-00462-0.

Chen H, Xu C, Yu Q, Zhong C, Peng Y, Chen J, Chen G. 2021a. Comprehensive landscape of STEAP family functions and prognostic prediction value in glioblastoma. *Journal of Cellular Physiology* **236**(4):2988–3000 DOI 10.1002/jcp.30060.

Costello JF, Fruhwald MC, Smiraglia DJ, Rush LJ, Robertson GP, Gao X, Wright FA, Feramisco JD, Peltomaki P, Lang JC, Schuller DE, Yu L, Bloomfield CD, Caligiuri MA, Yates A, Nishikawa R, Su Huang H, Petrelli NJ, Zhang X, O'Dorisio MS, Held WA, Cavenee WK, Plass C. 2000. Aberrant CpG-Island methylation has non-random and tumour-type-specific patterns. *Nature Genetics* **24**(2):132–138 DOI 10.1038/72785.

de Souza I, Monteiro LKS, Guedes CB, Silva MM, Andrade-Tomaz M, Contieri B, Latancia MT, Mendes D, Porchia B, Lazarini M, Gomes LR, Rocha CRR. 2022a. High levels of NRF2 sensitize temozolomide-resistant glioblastoma cells to ferroptosis via ABCC1/MRP1 upregulation. *Cell Death & Disease* **13**(7):591 DOI 10.1038/s41419-022-05044-9.

de Souza I, Ramalho MCC, Guedes CB, Osawa IYA, Monteiro LKS, Gomes LR, Rocha CRR. 2022b. Ferroptosis modulation: potential therapeutic target for glioblastoma treatment. *International Journal of Molecular Sciences* **23**(13):6879 DOI 10.3390/ijms23136879.

Fu J, Li K, Zhang W, Wan C, Zhang J, Jiang P, Liu XS. 2020. Large-scale public data reuse to model immunotherapy response and resistance. *Genome Medicine* **12**(1):21 DOI 10.1186/s13073-020-0721-z.

Guo Y, Li Y, Li J, Tao W, Dong W. 2021. DNA methylation-driven genes for developing survival nomogram for low-grade glioma. *Frontiers in Oncology* **11**:629521 DOI 10.3389/fonc.2021.629521.

Hambardzumyan D, Gutmann DH, Kettenmann H. 2016. The role of microglia and macrophages in glioma maintenance and progression. *Nature Neuroscience* **19**(1):20–27 DOI 10.1038/nn.4185.

Han M, Xu R, Wang S, Yang N, Ni S, Zhang Q, Xu Y, Zhang X, Zhang C, Wei Y, Ji J, Huang B, Zhang D, Chen A, Li W, Bjerkvig R, Li X, Wang J. 2018. Six-transmembrane epithelial antigen of prostate 3 predicts poor prognosis and promotes glioblastoma growth and invasion. *Neoplasia* **20**(6):543–554 DOI 10.1016/j.neo.2018.04.002.

Hu Z, Mi Y, Qian H, Guo N, Yan A, Zhang Y, Gao X. 2020. A potential mechanism of temozolomide resistance in glioma-ferroptosis. *Frontiers in Oncology* **10**:897 DOI 10.3389/fonc.2020.00897.

Huang HS, Su HY, Li PH, Chiang PH, Huang CH, Chen CH, Hsieh MC. 2018. Prognostic impact of tumor infiltrating lymphocytes on patients with metastatic urothelial carcinoma receiving platinum based chemotherapy. *Scientific Reports* **8(1)**:7485 DOI 10.1038/s41598-018-25944-1.

Jackson CM, Choi J, Lim M. 2019. Mechanisms of immunotherapy resistance: lessons from glioblastoma. *Nature Immunology* **20(9)**:1100–1109 DOI 10.1038/s41590-019-0433-y.

Klutstein M, Moss J, Kaplan T, Cedar H. 2017. Contribution of epigenetic mechanisms to variation in cancer risk among tissues. *Proceedings of the National Academy of Sciences of the United States of America* **114(9)**:2230–2234 DOI 10.1073/pnas.1616556114.

Kraehenbuehl L, Weng CH, Eghbali S, Wolchok JD, Merghoub T. 2022. Enhancing immunotherapy in cancer by targeting emerging immunomodulatory pathways. *Nature Reviews Clinical Oncology* **19(1)**:37–50 DOI 10.1038/s41571-021-00552-7.

Lei G, Zhuang L, Gan B. 2022. Targeting ferroptosis as a vulnerability in cancer. *Nature Reviews Cancer* **22(7)**:381–396 DOI 10.1038/s41568-022-00459-0.

Li T, Fu J, Zeng Z, Cohen D, Li J, Chen Q, Li B, Liu XS. 2020. TIMER2.0 for analysis of tumor-infiltrating immune cells. *Nucleic Acids Research* **48(W1)**:W509–W514 DOI 10.1093/nar/gkaa407.

Lim M, Xia Y, Bettegowda C, Weller M. 2018. Current state of immunotherapy for glioblastoma. *Nature Reviews Clinical Oncology* **15(7)**:422–442 DOI 10.1038/s41571-018-0003-5.

Liu J, Song X, Kuang F, Zhang Q, Xie Y, Kang R, Kroemer G, Tang D. 2021. NUPR1 is a critical repressor of ferroptosis. *Nature Communications* **12(1)**:647 DOI 10.1038/s41467-021-20904-2.

Liu S, Zhang C, Maimela NR, Yang L, Zhang Z, Ping Y, Huang L, Zhang Y. 2019. Molecular and clinical characterization of CD163 expression via large-scale analysis in glioma. *Oncoimmunology* **8(7)**:1601478 DOI 10.1080/2162402X.2019.1601478.

Louis DN, Perry A, Wesseling P, Brat DJ, Cree IA, Figarella-Branger D, Hawkins C, Ng HK, Pfister SM, Reifenberger G, Soffietti R, von Deimling A, Ellison DW. 2021. The 2021 WHO classification of tumors of the central nervous system: a summary. *Neuro Oncology* **23(8)**:1231–1251 DOI 10.1093/neuonc/noab106.

Lu J, Huang Y, Zhang X, Xu Y, Nie S. 2021. Noncoding RNAs involved in DNA methylation and histone methylation, and acetylation in diabetic vascular complications. *Pharmacological Research* **170**:105520 DOI 10.1016/j.phrs.2021.105520.

Magalhaes M, Manadas B, Efferth T, Cabral C. 2021. Chemoprevention and therapeutic role of essential oils and phenolic compounds: modeling tumor microenvironment in glioblastoma. *Pharmacological Research* **169**:105638 DOI 10.1016/j.phrs.2021.105638.

Ohgami RS, Campagna DR, Greer EL, Antiochos B, McDonald A, Chen J, Sharp JJ, Fujiwara Y, Barker JE, Fleming MD. 2005. Identification of a ferrireductase required for efficient transferrin-dependent iron uptake in erythroid cells. *Nature Genetics* **37(11)**:1264–1269 DOI 10.1038/ng1658.

Ohgami RS, Campagna DR, McDonald A, Fleming MD. 2006. The Steap proteins are metalloreductases. *Blood* **108(4)**:1388–1394 DOI 10.1182/blood-2006-02-003681.

Pathania R, Ramachandran S, Elangovan S, Padia R, Yang P, Cinghu S, Veeranan-Karmegam R, Arjunan P, Gnana-Prakasam JP, Sadanand F, Pei L, Chang CS, Choi JH, Shi H, Manicassamy S, Prasad PD, Sharma S, Ganapathy V, Jothi R, Thangaraju M.

2015. DNMT1 is essential for mammary and cancer stem cell maintenance and tumorigenesis. *Nature Communications* **6(1)**:6910 DOI 10.1038/ncomms7910.

Pogribna M, Hammons G. 2021. Epigenetic effects of nanomaterials and nanoparticles. *Journal of Nanobiotechnology* **19**:1–18 DOI 10.1186/s12951-020-00740-0.

Przystal JM, Becker H, Canjuga D, Tsiami F, Anderle N, Keller AL, Pohl A, Ries CH, Schmittnaegel M, Korinetska N, Koch M, Schittenhelm J, Tatagiba M, Schmees C, Beck SC, Tabatabai G. 2021. Targeting CSF1R alone or in combination with PD1 in experimental glioma. *Cancer* **13(10)**:2400 DOI 10.3390/cancers13102400.

Pyonteck SM, Akkari L, Schuhmacher AJ, Bowman RL, Sevenich L, Quail DF, Olson OC, Quick ML, Huse JT, Teijeiro V, Setty M, Leslie CS, Oei Y, Pedraza A, Zhang J, Brennan CW, Sutton JC, Holland EC, Daniel D, Joyce JA. 2013. CSF-1R inhibition alters macrophage polarization and blocks glioma progression. *Nature Medicine* **19(10)**:1264–1272 DOI 10.1038/nm.3337.

Qu C, Peng Y, Liu S. 2022. Ferroptosis biology and implication in cancers. *Frontiers in Molecular Biosciences* **9**:892957 DOI 10.3389/fmolb.2022.892957.

Ru B, Wong CN, Tong Y, Zhong JY, Zhong SSW, Wu WC, Chu KC, Wong CY, Lau CY, Chen I, Chan NW, Zhang J. 2019. TISIDB: an integrated repository portal for tumor-immune system interactions. *Bioinformatics* **35(20)**:4200–4202 DOI 10.1093/bioinformatics/btz210.

Russo G, Tramontano A, Iodice I, Chiariotti L, Pezone A. 2021. Epigenome chaos: stochastic and deterministic DNA methylation events drive cancer evolution. *Cancers* **13**:1800 DOI 10.3390/cancers13081800.

Sun Q, Xu Y, Yuan F, Qi Y, Wang Y, Chen Q, Liu B. 2022. Rho family GTPase 1 (RND1), a novel regulator of p53, enhances ferroptosis in glioblastoma. *Cell and Bioscience* **12(1)**:53 DOI 10.1186/s13578-022-00791-w.

Thorbinson C, Kilday J-P. 2021. Childhood malignant brain tumors: balancing the bench and bedside. *Cancers* **13**:6099 DOI 10.3390/cancers13236099.

Tsoi J, Robert L, Paraiso K, Galvan C, Sheu KM, Lay J, Wong DJL, Atefi M, Shirazi R, Wang X, Braas D, Grasso CS, Palaskas N, Ribas A, Graeber TG. 2018. Multi-stage differentiation defines melanoma subtypes with differential vulnerability to drug-induced iron-dependent oxidative stress. *Cancer Cell* **33(5)**:890–904.e5 DOI 10.1016/j.ccell.2018.03.017.

Uhlen M, Zhang C, Lee S, Sjostedt E, Fagerberg L, Bidkhori G, Benfeitas R, Arif M, Liu Z, Edfors F, Sanli K, von Feilitzen K, Oksvold P, Lundberg E, Hober S, Nilsson P, Mattsson J, Schwenk JM, Brunnstrom H, Glimelius B, Sjoblom T, Edqvist PH, Djureinovic D, Micke P, Lindskog C, Mardinoglu A, Ponten F. 2017. A pathology atlas of the human cancer transcriptome. *Science* **357(6352)**:1 DOI 10.1126/science.aan2507.

Vasaikar SV, Straub P, Wang J, Zhang B. 2018. LinkedOmics: analyzing multi-omics data within and across 32 cancer types. *Nucleic Acids Research* **46(D1)**:D956–D963 DOI 10.1093/nar/gkx1090.

Viswanathan VS, Ryan MJ, Dhruv HD, Gill S, Eichhoff OM, Seashore-Ludlow B, Kaffenberger SD, Eaton JK, Shimada K, Aguirre AJ, Viswanathan SR, Chattopadhyay S, Tamayo P, Yang WS, Rees MG, Chen S, Boskovic ZV, Javaid S, Huang C, Wu X, Tseng YY, Roider EM, Gao D, Cleary JM, Wolpin BM, Mesirov JP, Haber DA, Engelman JA, Boehm JS, Kotz JD, Hon CS, Chen Y, Hahn WC, Levesque MP, Doench JG, Berens ME, Shamji AF, Clemons PA, Stockwell BR, Schreiber SL. 2017. Dependency of a therapy-resistant state of cancer cells on a lipid peroxidase pathway. *Nature* **547(7664)**:453–457 DOI 10.1038/nature23007.

Wang K, Wang J, Zhang J, Zhang A, Liu Y, Zhou J, Wang X, Zhang J. 2022. Ferroptosis in glioma immune microenvironment: opportunity and challenge. *Frontiers in Oncology* 12:917634 DOI 10.3389/fonc.2022.917634.

Wei J, Marisetty A, Schrand B, Gabrusiewicz K, Hashimoto Y, Ott M, Grami Z, Kong LY, Ling X, Caruso H, Zhou S, Wang YA, Fuller GN, Huse J, Gilboa E, Kang N, Huang X, Verhaak R, Li S, Heimberger AB. 2019. Osteopontin mediates glioblastoma-associated macrophage infiltration and is a potential therapeutic target. *Journal of Clinical Investigation* 129(1):137–149 DOI 10.1172/JCI121266.

Weston C, Klobusicky J, Weston J, Connor J, Toms SA, Marko NF. 2016. Aberrations in the iron regulatory gene signature are associated with decreased survival in diffuse infiltrating gliomas. *PLOS ONE* 11(11):e0166593 DOI 10.1371/journal.pone.0166593.

Xia L, Gong M, Zou Y, Wang Z, Wu B, Zhang S, Li L, Jin K, Sun C. 2022. Apatinib induces ferroptosis of glioma cells through modulation of the VEGFR2/Nrf2 pathway. *Oxidative Medicine and Cellular Longevity* 2022(5):9925919 DOI 10.1155/2022/9925919.

Xu S, Tang L, Li X, Fan F, Liu Z. 2020. Immunotherapy for glioma: current management and future application. *Cancer Letters* 476:1–12 DOI 10.1016/j.canlet.2020.02.002.

Xu J, Yang X, Ji J, Gao Y, Qiu N, Xi Y, Liu A, Zhai G. 2021. RVG-functionalized reduction sensitive micelles for the effective accumulation of doxorubicin in brain. *Journal of Nanobiotechnology* 19:251 DOI 10.1186/s12951-021-00997-z.

Xue T, Qiu X, Liu H, Gan C, Tan Z, Xie Y, Wang Y, Ye T. 2021. Epigenetic regulation in fibrosis progress. *Pharmacological Research* 173:105910 DOI 10.1016/j.phrs.2021.105910.

Yan Y, Liang Q, Xu Z, Huang J, Chen X, Cai Y, Peng B, Yi Q. 2021. Downregulated ferroptosis-related gene STEAP3 as a novel diagnostic and prognostic target for hepatocellular carcinoma and its roles in immune regulation. *Frontiers in Cell and Developmental Biology* 9:743046 DOI 10.3389/fcell.2021.743046.

Ye LF, Chaudhary KR, Zandkarimi F, Harken AD, Kinslow CJ, Upadhyayula PS, Dovas A, Higgins DM, Tan H, Zhang Y, Buonanno M, Wang TJC, Hei TK, Bruce JN, Canoll PD, Cheng SK, Stockwell BR. 2020. Radiation-induced lipid peroxidation triggers ferroptosis and synergizes with ferroptosis inducers. *ACS Chemical Biology* 15(2):469–484 DOI 10.1021/acschembio.9b00939.

Yi Q, Liang Q, Liu Y, Gong Z, Yan Y. 2022. Application of genomic selection and experimental techniques to predict cell death and immunotherapeutic efficacy of ferroptosis-related CXCL2 in hepatocellular carcinoma. *Frontiers in Oncology* 12:998736 DOI 10.3389/fonc.2022.998736.

Yoshihara K, Shahmoradgoli M, Martinez E, Vegesna R, Kim H, Torres-Garcia W, Trevino V, Shen H, Laird PW, Levine DA, Carter SL, Getz G, Stemke-Hale K, Mills GB, Verhaak RG. 2013. Inferring tumour purity and stromal and immune cell admixture from expression data. *Nature Communications* 4(1):2612 DOI 10.1038/ncomms3612.

Yuan H, Yan M, Zhang G, Liu W, Deng C, Liao G, Xu L, Luo T, Yan H, Long Z, Shi A, Zhao T, Xiao Y, Li X. 2019. CancerSEA: a cancer single-cell state atlas. *Nucleic Acids Research* 47(D1):D900–D908 DOI 10.1093/nar/gky939.

Zhang Y, Guo P, Ma Z, Lu P, Kebebe D, Liu Z. 2021b. Combination of cell-penetrating peptides with nanomaterials for the potential therapeutics of central nervous system disorders: a review. *Journal of Nanobiotechnology* 19:1–22 DOI 10.1186/s12951-021-01002-3.

Zhang H, Luo YB, Wu W, Zhang L, Wang Z, Dai Z, Feng S, Cao H, Cheng Q, Liu Z. 2021a. The molecular feature of macrophages in tumor immune microenvironment of glioma patients. *Computational and Structural Biotechnology Journal* 19:4603–4618 DOI 10.1016/j.csbj.2021.08.019.

Zhao Z, Wang Z, Song Z, Wu Y, Jin Q, Zhao Z. 2021a. Predictive potential of STEAP family for survival, immune microenvironment and therapy response in glioma. *International Immunopharmacology* **101(5)**:108183 DOI 10.1016/j.intimp.2021.108183.

Zhao Z, Zhang KN, Wang Q, Li G, Zeng F, Zhang Y, Wu F, Chai R, Wang Z, Zhang C, Zhang W, Bao Z, Jiang T. 2021b. Chinese glioma genome atlas (CGGA): a comprehensive resource with functional genomic data from Chinese glioma patients. *Genomics, Proteomics & Bioinformatics* **19(1)**:1–12 DOI 10.1016/j.gpb.2020.10.005.